Natural Resources Canada
Ressources naturelles Canada

Lithospheric geometry revealed by deep-probing magnetotelluric surveying, Melville Peninsula, Nunavut

J. Spratt, A.G. Jones, D. Corrigan, and C. Hogg

Geological Survey of Canada
Current Research 2013-12

2013

Canada

Geological Survey of Canada
Current Research 2013-12

Lithospheric geometry revealed by deep-probing magnetotelluric surveying, Melville Peninsula, Nunavut

J. Spratt, A.G. Jones, D. Corrigan, and C. Hogg

2013

ISSN 1701-4387
Catalogue No. M44-2013/12E-PDF
ISBN 978-1-100-22156-4
doi:10.4095/292482

A copy of this publication is also available for reference in depository libraries across Canada through access to the Depository Services Program's Web site at http://dsp-psd.pwgsc.gc.ca

This publication is available for free download through GEOSCAN http://geoscan.ess.nrcan.gc.ca

Recommended citation

Spratt, J., Jones, A.G., Corrigan, D., and Hogg, C., 2013. Lithospheric geometry revealed by deep-probing magnetotelluric surveying, Melville Peninsula, Nunavut; Geological Survey of Canada, Current Research 2013-12, 14 p. doi:10.4095/292482

Critical review
J. Craven

Authors
J. Spratt (jessicaspratt@sympatico.ca)
49 Ch Mahon Sud
P.O. Box 136
La Peche, Quebec
H0X 3G0

A.G. Jones (alan@cp.dias.ie)
C. Hogg (chogg@cp.dias.ie)
Dublin Institute for Advanced Studies
School of Cosmic Physics
5 Merrion Square
Dublin 2, Ireland

D. Corrigan
(David.Corrigan@NRCan-RNCan.gc.ca)
Geological Survey of Canada
601 Booth Street
Ottawa, Ontario
K1A 0E8

Correction date:

Lithospheric geometry revealed by deep-probing magnetotelluric surveying, Melville Peninsula, Nunavut

J. Spratt, A.G. Jones, D. Corrigan, and C. Hogg

Spratt, J., Jones, A.G., Corrigan, D., and Hogg, C., 2013. Lithospheric geometry revealed by deep-probing magnetotelluric surveying, Melville Peninsula, Nunavut; Geological Survey of Canada, Current Research 2013-12, 14 p. doi:10.4095/292482

Abstract: As part of a multidisciplinary geoscience project, the conductivity structure of the lithosphere beneath the Melville Peninsula, Nunavut, has been imaged using lithosphere-probing magnetotelluric methods. Two-dimensional resistivity models demonstrate a strong correlation between the resistivity structure and features mapped at the surface. An analysis of distortion effects and structural dimensionality show that, toward the north at crustal depths, the geoelectric strike angle is 099° azimuth, consistent with abundant east-trending faults; however toward the south and at mantle depths the geoelectric strike direction is 034°, similar to the regional structural trend. The data reveal near-vertical, less resistive features that extend through the highly resistive Archean-age Prince Albert crustal block to the base of the crust and correlate with surface fault traces. Paleoproterozoic metasedimentary rocks of the Penrhyn Group are characteristic of extremely low resistivities associated with graphite-bearing metapelites. A near-vertical low resistivity zone is interpreted to represent a shear zone that marks the northern extent of the Archean Repulse Bay Block. Variations in the resistivity structure of the mantle lithosphere suggest changes in structure or composition between the Repulse Bay Block to the south and the Prince Albert Block to the north.

Resumé : Dans le cadre d'un projet géoscientifique multidisciplinaire, une représentation de la structure de conductivité de la lithosphère sous la presqu'île Melville (Nunavut) a été obtenue à l'aide de méthodes magnétotelluriques (MT) de sondage de la lithosphère. Des modèles bidimensionnels de la résistivité indiquent une forte corrélation entre la structure de résistivité et les entités cartographiées à la surface. Une analyse des effets de distorsion et de la dimensionnalité structurale montre que, vers le nord à des profondeurs crustales, l'azimut de la direction géoélectrique est de 099°, ce qui est cohérent avec l'abondance de failles orientées est-ouest. Cependant, vers le sud et aux profondeurs du manteau, l'azimut de la direction géoélectrique est de 034°, ce qui est similaire à celui de la direction structurale à l'échelle régionale. Les données montrent des entités moins résistives, presque verticales, qui traversent le bloc crustal hautement résistif de Prince Albert de l'Archéen jusqu'à la base de la croûte et qui peuvent être mises en corrélation avec les lignes de faille en surface. Les roches métasédimentaires du Groupe de Penrhyn du Paléoprotérozoïque sont caractéristiques des résistivités extrêmement faibles associées à des métapélites graphiteuses. Selon les interprétations, une zone presque verticale de faible résistivité représenterait une zone de cisaillement marquant la limite nord du bloc de Repulse Bay de l'Archéen. Des variations de la structure de résistivité de la lithosphère mantellique laissent supposer des changements dans la structure ou la composition entre le bloc de Repulse Bay au sud et le bloc de Prince Albert au nord.

INTRODUCTION

Melville Peninsula, mainland Nunavut, is located within the Rae Craton in the Churchill Province of the eastern Canadian Shield (Fig. 1), and contains geological and tectonic elements that are favourable for precious- and base-metal mineralization and the preservation of diamond-bearing kimberlite deposits. Limited studies have been previously undertaken to understand the geology and develop the exploration potential of the region. As part of the multidisciplinary Melville Peninsula Project under the Geo-Mapping for Minerals and Energy (GEM) Program (D. Corrigan, L. Nadeau, P. Brouillette, N. Wodicka, M. Houlé, T. Tremblay, G. Machado, and P. Keating, unpub. report, 2013), crustal-scale and deep penetrating magnetotelluric (MT) data were collected along a 300 km long, approximately north-south profile to image the subsurface conductivity structure of the lithosphere beneath the project area. The overarching objectives of the study were resolving the subsurface geometry of major crustal and upper mantle boundaries, providing insight on the structural evolution and tectonic processes, and developing an understanding of the potential for mineral exploitation in the region. The MT profile extends from the Archean Repulse Bay Block to the south, across the Paleoproterozoic Penrhyn Group and the Neoarchean Prince Albert Group into the Northern granulite block to the north (Fig. 2). Images of the resistivity structure of the crust and upper mantle beneath this regional profile derived from the magnetotelluric data reveal key information on the thickness, mineral composition, and electrical properties of the lithosphere.

GEOLOGICAL OVERVIEW

Archean rocks of Melville Peninsula, which forms part of the Rae Craton, contain variably reworked orthogneiss units (Frisch, 1980), metamorphosed sedimentary and volcanic rocks of the Prince Albert Group, as well as mafic to felsic plutonic rocks (Fig. 2). Granulite facies orthogneiss are found on the northern part of Melville Peninsula (Schau and Heywood, 1984). The northernmost tip of the peninsula contains Neoproterozoic gabbro, basalt, and clastic sedimentary rocks of the Mesoproterozoic Fury and Heckla Group, now preserved in south-dipping cuestas (Blackadar, 1958; Schau and Heywood, 1984). Northern Melville Peninsula

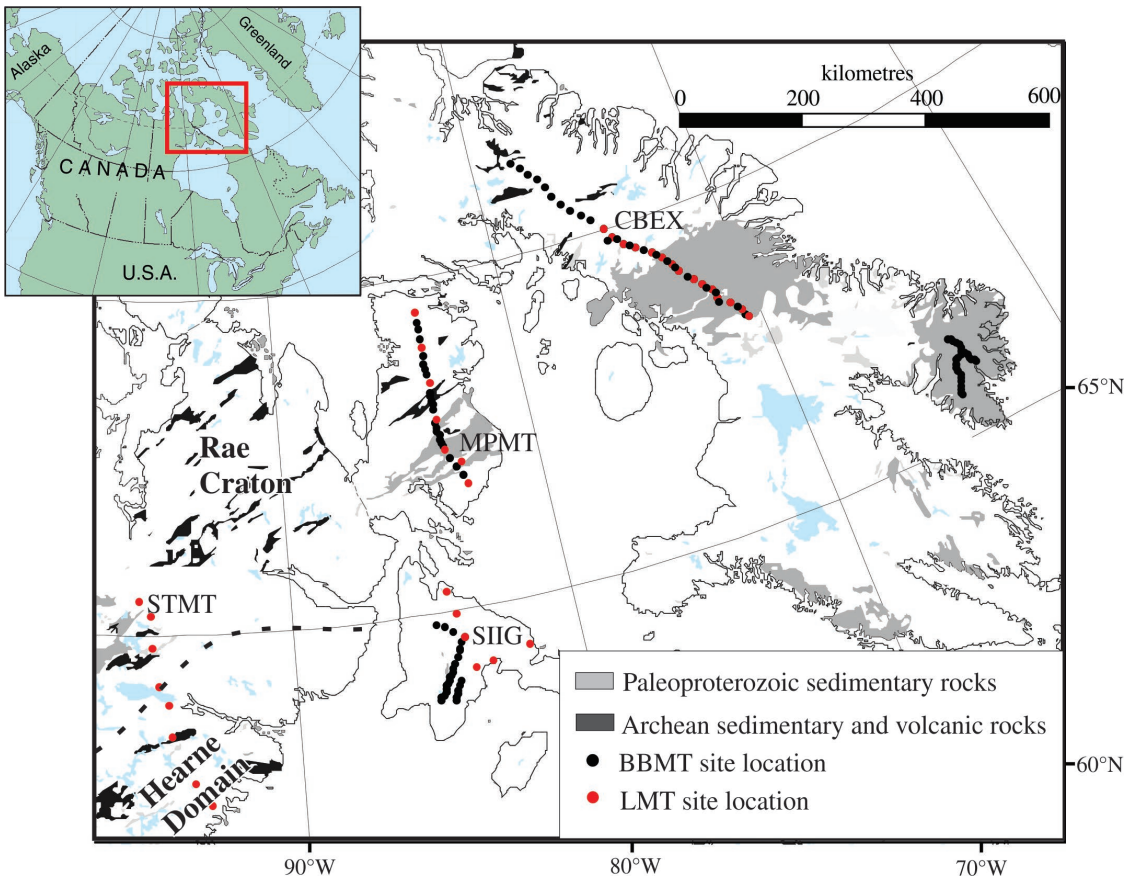

Figure 1. Regional map of the Churchill Province showing the location of the 'Melville Peninsula MT' survey (MPMT), the 'Central Baffin Electromagnetic Experiment' (CBEX), the 'Snowbird tectonic zone MT' (STMT) profile, and the 'Southampton Island Integrated Geoscience' MT project (SIIG).

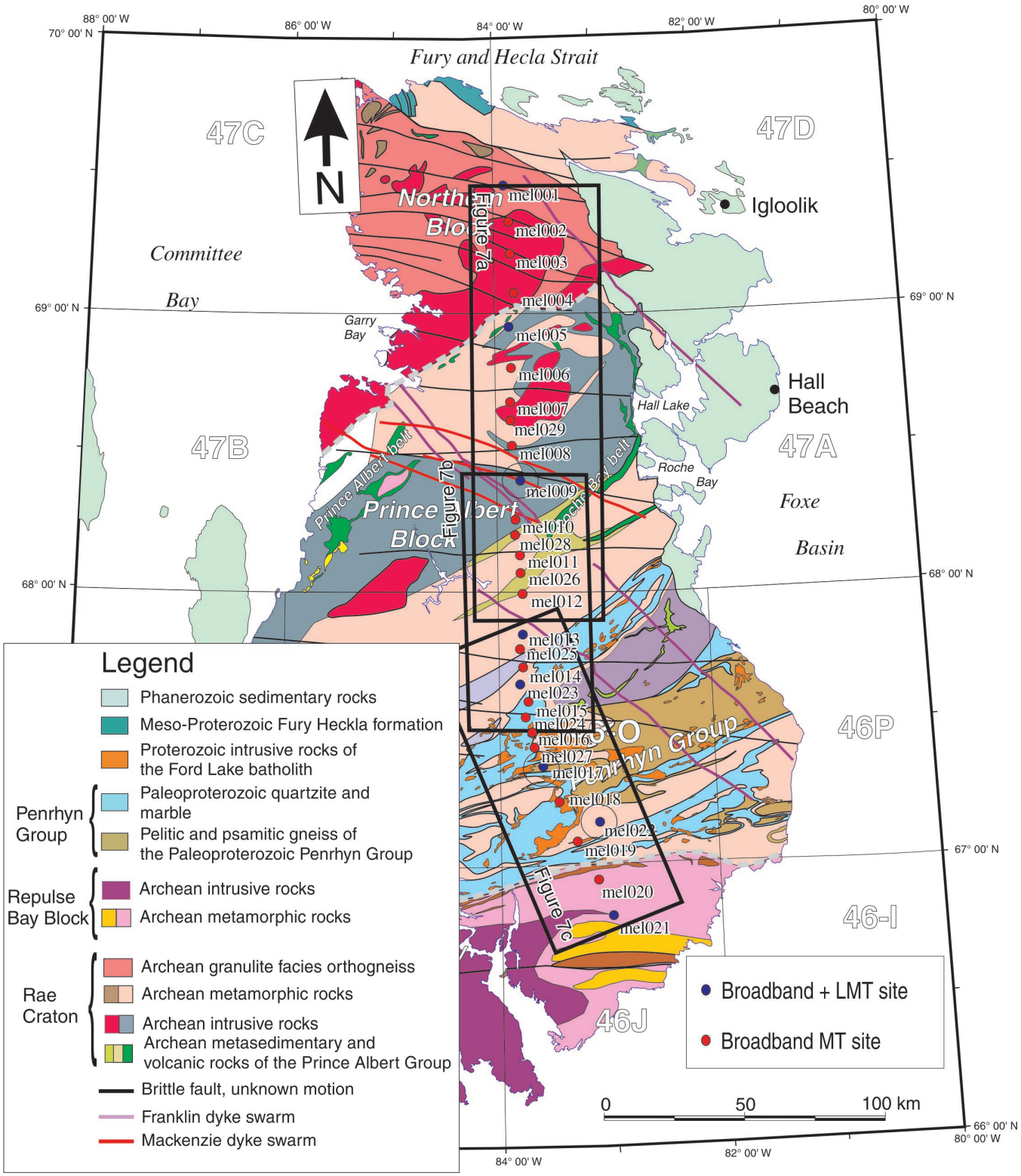

Figure 2. Geological map of the Melville Peninsula showing the location of the MT recording sites. The rectangles show the models sections in Figure 7. The circles mark the location of the response curves examples shown in Figure 4.

also hosts diamondiferous kimberlite deposits that intrude as sheet-like bodies concentrated along long-lived, east-west brittle faults. Paleozoic rocks, primarily limestone, flank the eastern margin of the peninsula and are locally reactivated by the east-west brittle faults.

The regional geological structure of Melville Peninsula has a northeast-trending fabric that is likely related to Paleoproterozoic deformation, perhaps initially from late-Archean to earliest Paleoproterozoic events and subsequently from the 1.88–1.80 Ga Trans-Hudson Orogen (Berman et al., 2005; Corrigan et al., 2009). Archean structures, more common in the northern third of the peninsula, seem to be striking along a more north-northeast trend. A series of east-trending brittle faults (Fig. 3) are mapped throughout Melville Peninsula; however, little information is known as to the depth extent, age, or direction of movement along these faults. North-trending, east-side-down, normal faults separating the Paleozoic rocks to the east are interpreted to be related to the opening of Baffin Bay.

The southern half of Melville Peninsula contains a series of Paleoproterozoic, metasedimentary, supracrustal rocks of the Penrhyn Group that occur in wide northeast- trending belts separated by basement inliers of presumably Archean gneiss (Fig. 2). The Penrhyn Group consists of interbedded successions of pelitic and psammitic gneiss, calc-silicate gneiss, marble, quartzite, and minor amphibolite (Henderson, 1983). Graphite is abundant in the pelitic gneiss and present in cleavages of the marble units along with some iron sulphide minerals. The belt of metasedimentary rocks contains economic occurrences of base-metal minerals and uranium (Henderson, 1983). The Penrhyn Group displays multiple stages of folding, defining the Fox fold belt, and comprises large basement-cored nappes (Henderson, 1983). These are intruded by 1.82 Ga monzogranite units that are part of the Hudson Suite (LeCheminant et al., 1987; Erdmann et al., 2013), all of which are cut by 1.1 Ga Mackenzie gabbro dykes.

Figure 3. Oblique aerial photograph of the western side of Melville Peninsula over the Prince Albert Hills, looking easterly. The picture shows one of the prominent set of brittle east-west oriented faults that transect the area. Photograph by D. Corrigan. 2013-107. Photograph taken on July 1st, 2011.

South of the Paleoproterozoic Penrhyn Group is the Repulse Bay Block that includes Archean orthogneiss (Laflamme, 2011). At the southernmost extent of the Melville Peninsula, the gneissic rocks include granulite facies orthogniess.

BACKGROUND AND PREVIOUS MAGETOTELLURIC STUDIES

The magetotelluric method (MT) provides information on the electrical resistivity of the subsurface of the Earth by measuring natural time-varying horizontal electric (E) and magnetic (H) fields at its surface (Cagniard, 1953; Wait, 1962; Jones, 1992). Typically plotted as MT response curves, the period-dependent apparent resistivities and phase lags are calculated from these measured time-varying fields over a broad period range. The depth to which the electric and magnetic fields penetrate (the skin depth effect) is dependent on their frequency and the conductivity of the layered Earth, therefore estimates of resistivity with depth can be made beneath each site recorded (Jones, 1983, 2006).

The MT method is sensitive to contrasts in the resistivity of different materials and can therefore distinguish between some lithological units and image structural features at depth. Typical Archean granulite facies, for example, commonly have high electrical resistivity values more than 1000 Ω·m (e.g. Wu et al., 2002), whereas sedimentary rocks are less resistive, with values ranging between 10 Ω·m and 1000 Ω·m. At crustal depths, factors that can considerably reduce typical resistivity values include changes in mineralogy, or the presences of saline fluids (Haak and Hutton, 1986; Jones, 1992).

Although its cause remain uncertain, lower-crustal reduced resistivity is observed over much of the continental lower crust (Jones, 1992) preventing the crust-mantle boundary from being detected by electromagnetic methods and complicating interpretations of the uppermost mantle (Jones (1999); Korja (2007) and references therein). The crust of western Slave Craton is one exception, where resistivity values of about 40 000 Ω·m are observed to several tens of kilometres (Jones et al., 2003), suggesting differences in the composition or tectonic processes involved in its formation. In the absence of a lower-crustal conductor, a decrease in resistivity, to values of about 4000 Ω·m, is observed at depths consistent with interpretations for the crust-mantle boundary, suggesting that the MT method is capable of indentifying the thickness of continental crust (Jones and Ferguson, 2001).

Typical values for the resistivity of mantle lithosphere are on the order of 5000–10 000 Ω·m and higher (Jones et al., 2009a). Reduced resistivity of several orders of magnitude

in the lithospheric mantle has been attributed to fluids or melt (Glover et al., 2000), or the presence of interconnected carbon, sulphide minerals or hydrous minerals (Duba and Shankland, 1982; Ducea and Park, 2000; Yoshino et al., 2009; Poe et al., 2010). A reduction in mantle olivine grain size has also been postulated to lower the resistivity by up to two orders of magnitude (ten Grotenhuis et al., 2004), due to grain-boundary conduction effects, making it possible to identify zones of mantle shearing using MT methods (e.g. Spratt et al., 2009). The MT method is useful in determining the electric lithosphere-asthenosphere boundary as there is a dramatic decrease in the resistivity value attributed to an increase in either free water or the onset of partial melt (Eaton et al., 2009 and references therein).

PREVIOUS MAGNETOTELLURIC STUDIES OF THE RAE CRATON

Magnetotelluric data have been previously used to image the lithospheric structure of the Churchill Province (Fig. 1). A combined MT and teleseismic survey across the Snowbird tectonic zone (STMT Jones et al., 2002) and MT survey across central Baffin Island (Central Baffin Electromagnetic Experiment: CBEX; Evans et al. (2003)) provide insight on the subsurface structure. These, along with the new Melville Peninsula profile, allow comparisons to be made on the regional conductivity structure of the Rae Craton.

In 1998, eight MT and teleseismic stations were collected across the snowbird tectonic zone, a Paleoproterozoic suture between the Hearne Domain and Rae Craton (Jones et al., 2002). Similar to the western Slave Craton, the Rae Craton was observed to be highly resistive (>10 000 Ω·m) through to the lower crust. It was interpreted that tectonic processes of lower crustal development in the Rae Craton and southwestern Slave Craton were similar, and different from processes that introduced low resistivity material into the lower crust of other Archean regions (Superior craton, Kaapvaal craton, *see* Jones, 1992). Due to extensive mantle metasomatism, low resistivities were expected for the subcontinental lithospheric mantle (SCLM) (Boerner et al., 1999); however, Jones et al. (2002) observed higher resistivities than beneath other cratons with values more than 60 000 Ω·m beneath the Rae Craton and about 6000 Ω·m beneath the Hearne Domain. A south-dipping boundary between the Rae Craton and Hearne Domain mantle properties was imaged.

In the early 2000s, a broadband and long period MT survey was conducted across central Baffin Island ("CBEX" of Evans et al., 2003). The 500 km long profile crosses Paleoproterozoic metasedimentary rocks of the Trans-Hudson Orogen Piling Group to the south onto the Archean Rae Craton to the north (Evans et al., 2005). A particular horizon within the Piling Group, the sulphidic-graphitic Astarte River formation, was found to be highly conductive due to the interconnected graphite. A strong resistivity contrast was observed between the Piling Group and the Archean granite and gneissic complexes of the Rae Craton to the north. The upper crustal Rae Craton rocks were found to be highly resistive (>10 000 Ω·m), however, contrary to the result of Jones et al. (2002), they found the lower crust of the Rae Craton to have moderately low resistivity values (~100 Ω·m). The upper mantle beneath the profile showed a resistive Archean mantle (>3000 Ω·m) beneath the Rae Craton and a moderately resistive Proterozoic mantle (~300 Ω·m) beneath the exposed Piling Group, with a south-dipping interface between the two.

DATA ACQUISITION AND ANALYSIS

During the 2009 summer field season, magnetotelluric (MT) data were collected at 29 site locations along a 300 km long profile extending from north to south across the Melville Peninsula (Fig. 1). Broadband MT (BBMT) period data, typically used to image crustal-scale features, were recorded for 2–3 days at each site at 15 km intervals and at higher densities across mapped geological boundaries using Phoenix Geophysics Limited, MTU-5A systems owned by the Geological Survey of Canada. Long period MT (LMT) data, used to image the deeper lithospheric structure, were recorded for three weeks at each site at 60 km intervals, as well as two selected locations in the south end of the profile, using Ukrainian built LEMI-417 instruments owned by the Dublin Institute for Advanced Studies (Ireland). Each MT site layout was composed of five lead-lead-chloride porous pot electrodes to measure the electric fields in two perpendicular directions. The broadband sites used two separate magnetic coils to measure the horizontal magnetic fields and, at some locations, an air loop to measure the vertical magnetic field. The long period sites recorded the three magnetic field components using a single three-component ring-core fluxgate magnetometer.

PROCESSING

The broadband data were processed from time series to response functions (apparent resistivity and phase curves) using robust remote reference techniques (Method 6 in Jones et al. (1989)), as implemented by the Phoenix Geophysics software package MT2000, and yielded apparent resistivity and phase response curves in the period range of 0.004– 1000 s for most sites along the profile. The long period data were processed using the multiremote-reference, robust, cascade decimation code of Jones (Jones and Jödicke, 1984) and the bounded-influence remote reference code of Chave (Chave and Thomson, 2004). The results were then merged with those from the broadband to obtain response curves that extend to greater periods. In general data quality is excellent with low error bars and smooth response curves that span up to eight decades of period, 0.004 to up to 20 000 s (Fig. 4). Initial observations of the processed response curves reveal consistently higher resistivities at the

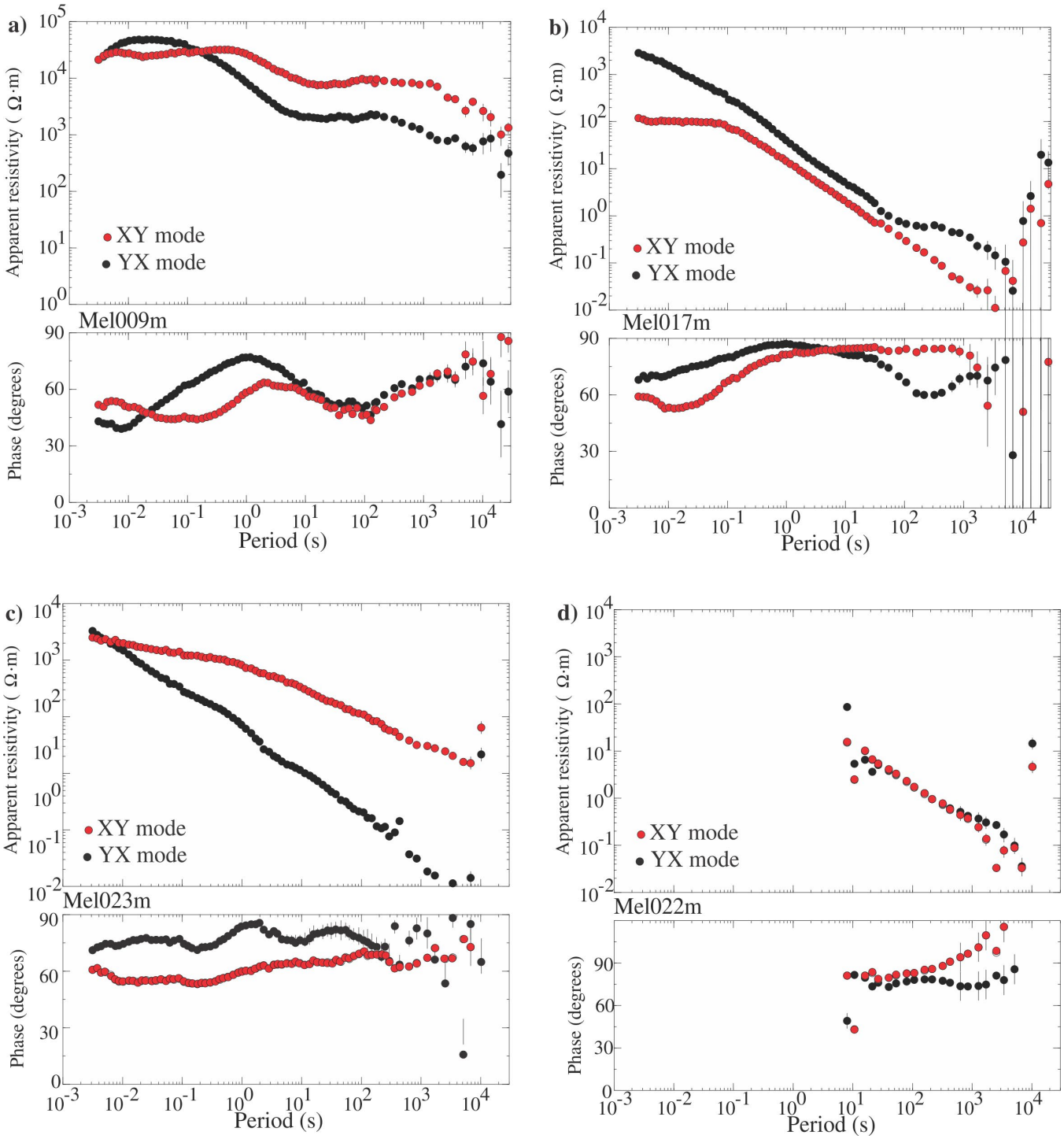

Figure 4. Examples of MT response curves for data measured at four sites: **a)** merged broadband and long period data at a site located within resistive Archean orthogneiss, **b)** data at a site located within the conductive Paleoproterozoic metasedimentary rocks, and **c)**, **d)** examples from sites located on pockets of Archean basement rocks between belts of Paleoproterozoic units.

northernmost sites (Fig. 4a) to long periods and therefore greater depths; however, the response curves for sites in the vicinity of the Penrhyn Group show enhanced conductivities to long periods (example Fig. 4b) limiting the depth of penetration. In an attempt to image deep structure beneath the Penrhyn Group, sites were installed on exposed basement rocks within the Fox fold belt, sites mel022 and mel023 (Fig. 4c, d). The results indicate steeply dropping apparent resistivities and phases that approach 90°, suggesting that although the near-surface material consists of resistive basement gneiss units, these are underlain by very low resistivities similar to those observed throughout the Penrhyn Group.

Nonuniform source field effects, due to the auroral electrojet, often cause distortion on MT data collected at high latitudes. Analyses using the method described in Jones and Spratt (2001) showed that there was little such effect on the long period data, perhaps due to the low solar activity at the time of recording.

DECOMPOSITION

In a layered isotropic Earth, i.e. where the Earth is considered one-dimensional (1-D), the apparent resistivities and phases at each period are independent of direction. In order to image resistivity structure that varies laterally along a profile, that is where the Earth is electrically two-dimensional (2-D), the apparent resistivity and phase response curves are calculated parallel to (termed the transverse-electric (TE) mode) and perpendicular to (transverse-magnetic (TM) mode) the geoelectric strike direction. At short periods, where the electromagnetic fields are penetrating the top few kilometres, geoelectric strike usually mimics geological strike. As period increases, i.e. depth penetration increases, then the geoelectric strike often rotates to other directions, indicative of the strike of subsurface structures and geometries that cannot be defined by surface mapping. Such variation can aid interpretation (*see*, for example Marquis et al., 1995).

The data were analyzed for the effects of galvanic distortions, the degree of dimensionality, and to determine the preferred geo-electric strike direction. Single site and multisite Groom Bailey decompositions (Groom and Bailey, 1989) were applied to each of the MT sites along the profile using the technique developed by McNeice and Jones (2001). The strike directions (with a 90° ambiguity) resulting from single-site, single-decade period-band decompositions are shown in Figure 5, where the colour scale represents the maximum phase difference between the TE and TM modes. Where the phase difference is minimal (<10°) the data can be considered approximately 1-D, or independent of the geoelectrical strike angle. Where the difference is greatest, the data are most dependent on the strike angle. In general, the sites at the southern end of the profile are predominantly 1-D over most of the period range. Where the phase differences are higher there is a strike preference of approximately 35–45°. The northernmost sites show a strong preference for a geoelectric strike angle of 9–17° at shorter periods (<1 s); however at longer periods (>1 s) there is a preference for 32–45°.

Estimates for the penetration depths at various periods were made using the Niblett-Bostick depth approximation (Niblett and Sayn-Wittgenstein, 1960; Bostick, 1977, Jones, 1983) and suggests that this change in geoelectric strike direction beneath the northern sites occurs at depths of about 30–40 km. This indicates that there are regional changes in the electrical structure at or close to the crust-mantle boundary. In the northernmost half of the profile, the regional geology is cut by a series of east-trending faults, likely influencing the geoelectric strike direction. As such, the TE mode is then perpendicular to the profile direction at −81°/+99°. These faults are not as predominant in the south where the shallow geoelectric strike direction (+34°) is parallel to the regional geological trends. The preferred strike angle of 34° for the deeper structure along the entire length of the profile is also similar to the regional geology. This indicates a coupling between the crust and mantle and suggests that the east-faulting observed to the north do not extend beyond the base of the crust.

Ideally, in a 2-D Earth, a single strike direction perpendicular to the site profile can be used to accurately model the responses at all periods for all sites. The data at each site were recalculated for both directions at all periods with an error floor of 3.5% (equivalent to 1° in phase, which is twice the calculated error level), to assess the sensitivity of data misfit with changes in the strike direction (Fig. 6a, b). At a strike of 9° higher error values (root mean square>3) are observed for periods greater than tens, whereas at a strike of 34° higher errors are seen at shorter periods, indicating that an accurate 2-D representation of the Earth cannot be made with a single geoelectric strike angle for all sites and all periods. Distortion-corrected data have been recalculated at both 9° and 34° and modelled separately at the appropriate period ranges. Three-dimensional inversion should be used to deal with depth and laterally-varying strike direction, but these are in their infancy and are not yet sufficiently developed to be useful as a reliable geological tool for regional studies.

DEPTH PENETRATION

An estimate of the maximum depth penetration beneath each site was determined using Schmucker's C-function conversion (Schmucker, 1970). These estimations infer that, in the north where the subsurface is resistive, penetration more than 200 km (Fig. 6c) is obtained and in some cases over 400 km. These depths are sufficient to model mantle lithospheric features. In the south, however, penetration through the conductive Penrhyn Group is limited to less than 30 km, but the EM fields at the southernmost sites reach depths of more than 100 km. As the area over which the apparent resistivity is averaged increases with depth beneath each site, it

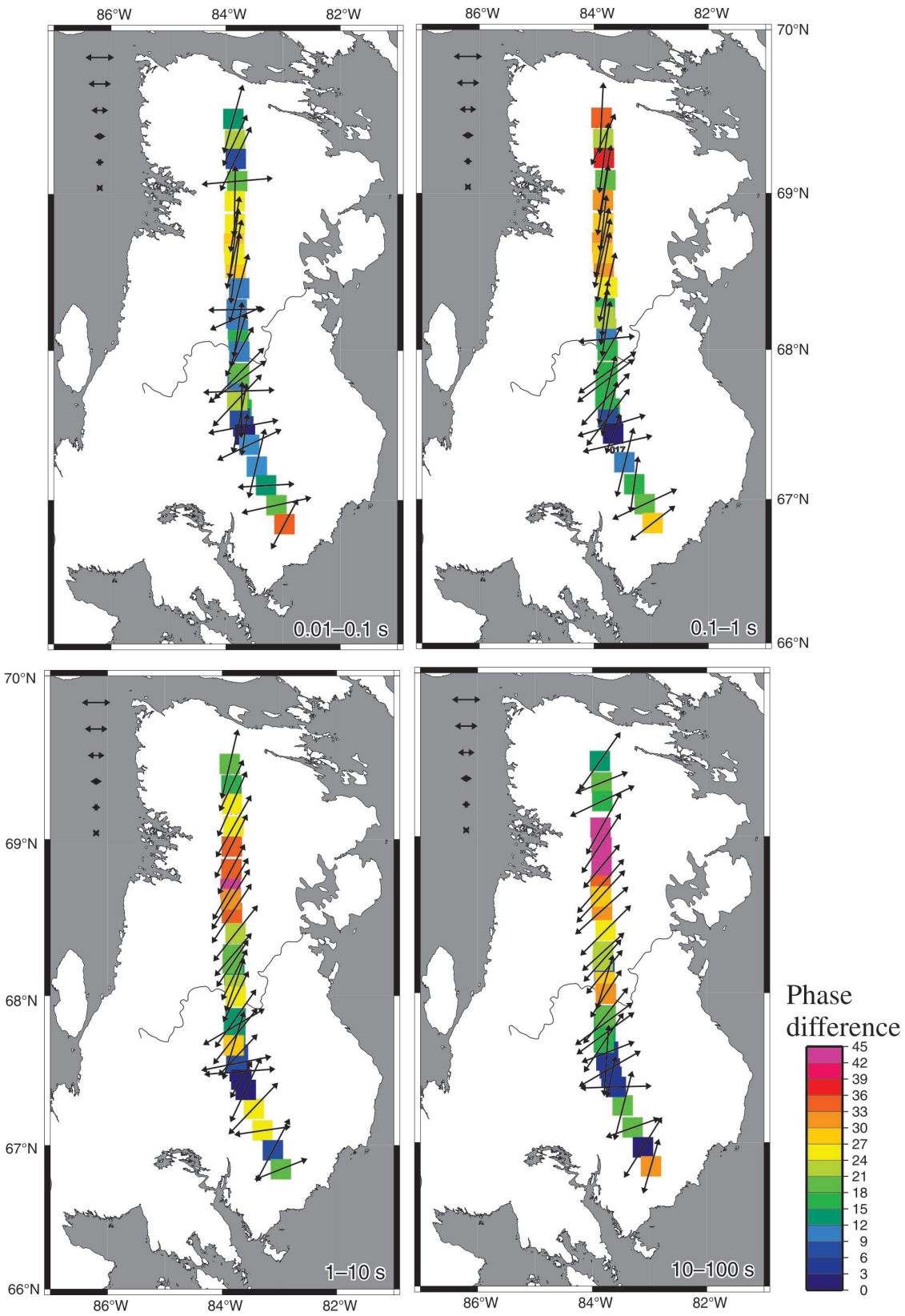

Figure 5. Maps showing the preferred geoelectric strike direction at each site along the profile for four decade period bands. The colour scale illustrates the maximum difference between the TM- and TE-mode phases.

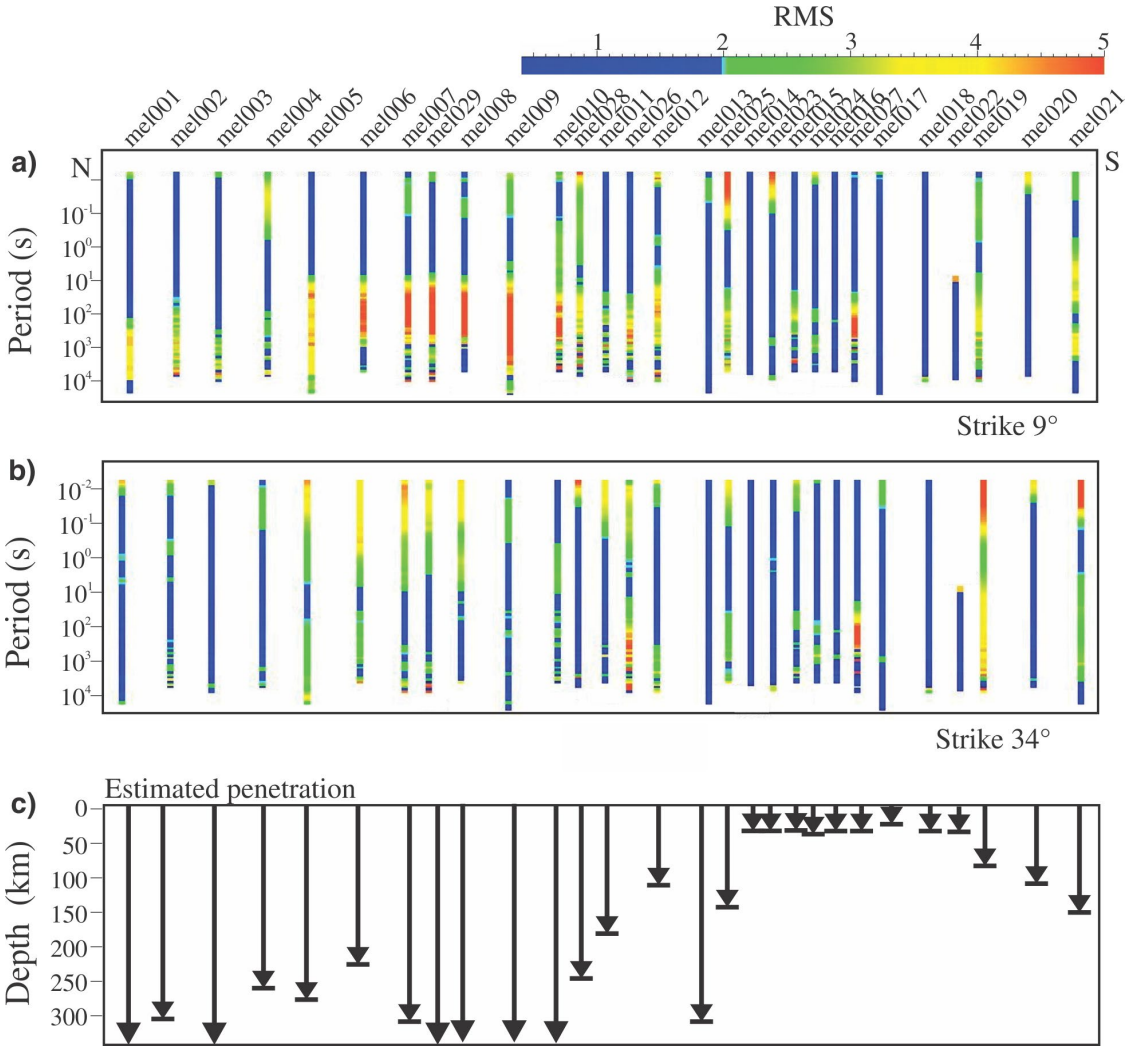

Figure 6. Data misfit values at each site over the whole recorded period range for data recalculated at a geoelectric strike direction of **a)** 9° and **b)** 34°. **c)** Penetration depth estimates for each site along the profile. RMS = root mean square

is possible that some deep structure beneath the Penrhyn Group may be resolved; however, extensive model testing is required to determine the reliability of the models.

OCEAN EFFECTS

An attempt to determine the distortion effects resulting from the presence of conductive sea water around the entire profile was made using the 3-D module of the WinGLink interpretation software package. A 3-D mesh was created, where the land cells had a uniform conductivity value of 500 Ω·m and the cells representing the approximate location and depth of the sea water surrounding the Melville Peninsula were added with a conductivity value of 0.1 Ω·m. A forward calculation of the response curves showed that the sites furthest from the coast were mildly influenced by the presence of the sea water at periods greater than 1000 s. The sites closest to the coast, particularly to the west where the sea is deeper, showed an effect as early as 300 s. As a uniform Earth was used and not the true conductivity structure of Melville Peninsula, this is an approximation and although maximum periods were used to generate the 2-D models, features resulting from periods greater than 1000 s need to be carefully examined.

PRELIMINARY 2-D MODELS AND INTERPRETATIONS

Two-dimensional models were generated using the WinGlink intepretation software package. Inversions were undertaken using varying starting models, varying modelling parameters, and different combinations of data inputs and over 100 iterations were executed to obtain the final models. The data at periods that image crustal depths have

been divided into three (northern, middle, and southern) profiles in an attempt to obtain higher resolution of the local conductivity structure and to account for varying strike angles (Fig. 7). The crustal-scale models used data from the TM- and TE-modes as well as where available the vertical field transfer function in the period range of 0.004–10 s from the broadband MT sites. Error floors, determined acceptable from decomposition analysis, were set at 7% for both the phases and apparent resistivities and the smoothing parameter, tau, was set to seven (determined after initial trial runs with varying tau). In order to assess model feature differences with varying strike angles, forward inversions for each profile were undertaken at a geoelectric strike angle of +99° and +34°, as determined from the decomposition analysis. Additionally, a model has been generated using the data from all sites to periods of 10 000 s at a strike angle of 34° to image the regional lithospheric structure (Fig. 8).

CRUSTAL IMAGES

The northernmost profile, modelled at a geoelectric strike angle of +99°, obtained a minimum root mean square (RMS) misfit of 1.8 (Fig. 7a). In general the northern half of the Melville Peninsula is highly resistive (>10 000 Ω·m), consistent with values observed for the Rae Craton along two earlier MT profiles (Jones et al., 2002; Evans et al., 2005). In contrast to typical worldwide observations, the high resistivities are imaged through to lower crustal depths. These results are similar to those of Jones et al. (2002) near the Rae Craton–Hearne Domain boundary, but differ from the Evans et al. (2005) models generated beneath Baffin Island. A moderate decrease in resistivity is revealed at depths between 36 km and 39 km, marked by a dashed yellow line in Figure 7a, and is interpreted to represent the crust-mantle boundary. This increase is similar to the resistivity values estimated for the upper mantle beneath the western Slave Craton, where resistive lower crustal values are also observed. Throughout the northern profile, less resistive near-vertical structures

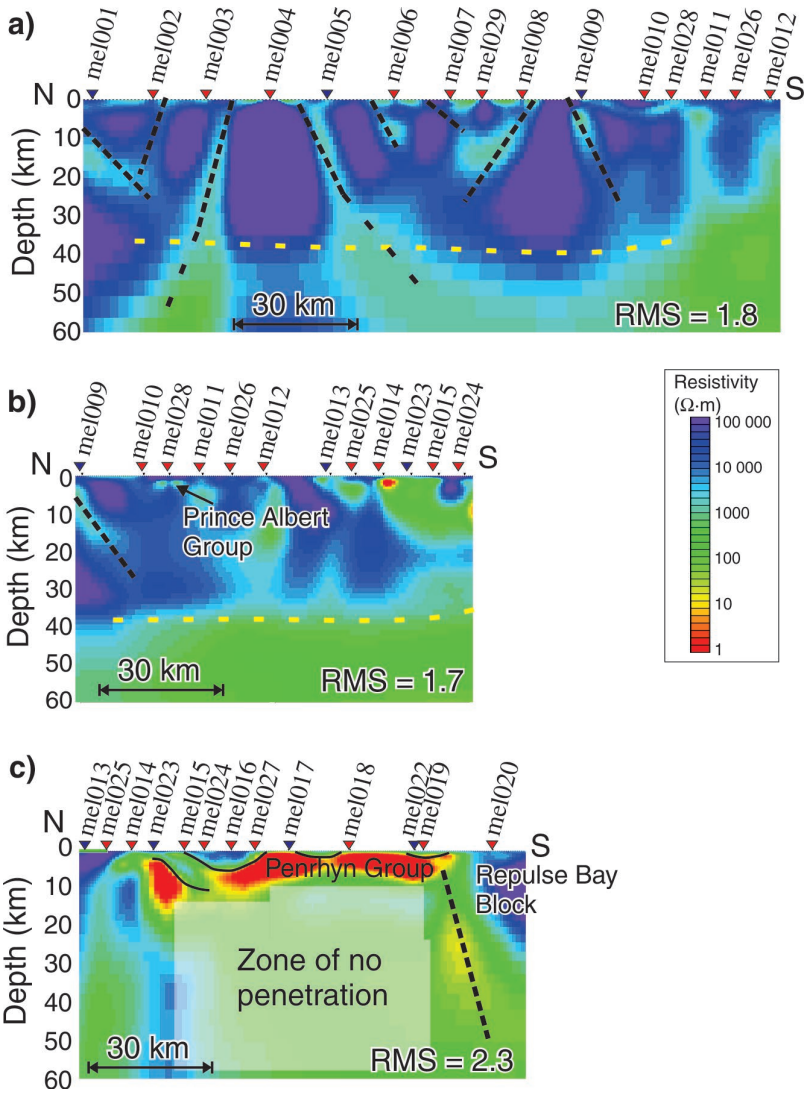

Figure 7. Two-dimensional conductivity models along the Melville Peninsula MT profile, divided into three sections: **a)** north, **b)** mid, and **c)** south. The yellow dashed line illustrates the interpreted crust mantle boundary. The black dashed lines mark the subsurface trace of faults mapped at the surface. The black arrow in Figure 7b marks possible folding of the Prince Albert Group. The black solid line marks the top of the graphite-bearing metasedimentary units of the Penhryn Group. RMS = root mean square

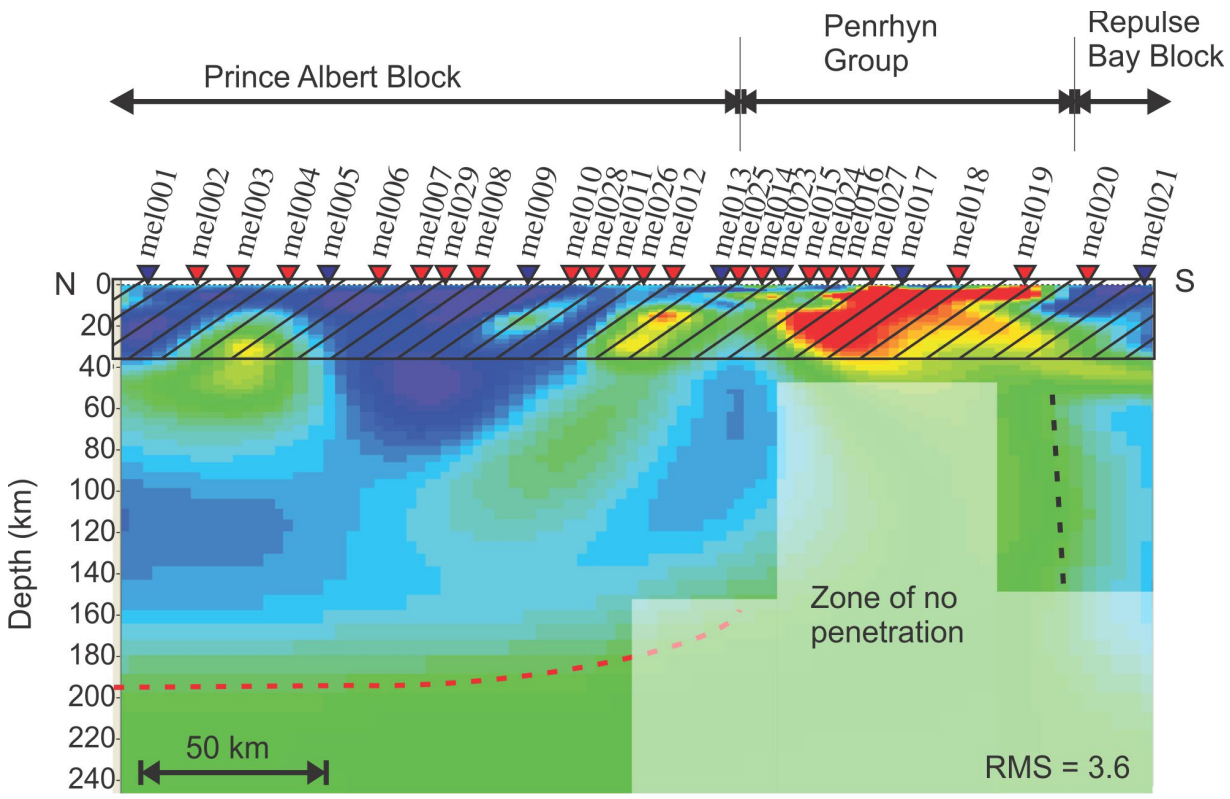

Figure 8. Conductivity structure of the upper mantle beneath the Melville Peninsula MT profile. The dashed red line marks the boundary between the lithosphere and underlying asthenosphere. The black dashed line marks a change in the lateral conductivity of the upper mantle.

are imaged that spatially correlate with east-trending faults mapped at the surface. Many of these faults appear to extend through to the base of the crust. At least one of these faults, which intersects the surface about 5 km south of site mel003, may extend into the uppermost mantle. This fault is in the vicinity of a known diamondiferous kimberlite field and may provide key information on the tectonic history of the region and diamond emplacement mechanisms.

The middle subprofile, modelled at a geoelectric strike of +99°, obtained a minimum root mean square misfit of 1.7 (Fig. 7b). Similar to the northern profile, high resistivities are seen to depths of 36–39 km, where there is a decrease from more than 10 000 Ω·m to about 4000 Ω·m interpreted as the crust-mantle boundary. In the vicinity of surface mapped Prince Albert Group there is a shallow, less resistive region that shows evidence of folding beneath the surface. The resistivity values are similar to those observed in the near-vertical faults, but the geometry of the body is different.

The southern profile, modelled at a strike of 34°, reached a minimum root mean square misfit of 2.3 (Fig. 7c). In contrast to the northern profile, the shallow southern section is marked by exceedingly low resistivity values (<10 Ω·m). The low resistivities are interpreted to result from the presence of abundant graphite in the supracrustal pelitic gneiss units of the Penrhyn Group. This unit is laterally continuous for about 80 km and appears to form a synclinal structure beneath sites mel015, mel024, and mel016, with resistive material near the surface. The lateral continuity and general geometry is consistent with the interpretations of Henderson (1983), where the exposed basement complexes were interpreted as structural nappes rather than windows into the underlying basement. The low resistivities cause attenuation of the amplitudes of the electric and magnetic fields, preventing penetration deep into the lower crust.

Several sensitivity tests were undertaken to assess the depths to which the model can be considered reliable. This was performed by altering the resistivity values of the cells directly beneath the low resistivity zone, running a forward inversion, and noting the change in root mean squares misfit value between the calculated and measured responses. In all cases, the root mean squares value did not show a significant increase for changes to the model between 7 km and 70 km, suggesting that the data are not sensitive to structure at these depths. The southern edge of the exposed Penrhyn Group is marked by a near-vertical conductor that extends to at least 50 km in depth. Sensitivity tests similar to those described above were conducted to determine the reliability of this low resistivity anomaly. In this case, the root mean square value increased to 3.2 suggesting that this feature is required by the data. This structural feature is interpreted to represent mineralization within a crustal-scale fault.

MANTLE IMAGES

The conductivity structure of the mantle was modelled along the whole profile at a strike angle of 34°, and used data in the period range of 1–10 000 s. The final model obtained a root mean square misfit value of 3.6 (Fig. 8). The effects of nearby sea water have not been taken into account; therefore, the deep mantle images are preliminary and need to be verified with 3-D modelling. Large-scale lateral changes of electrical resistivity within the upper mantle are observed. Beneath most of the profile, the mantle lithosphere has resistivity values of about 5000 Ω·m to depths of about 200 km, where there is a decrease in resistivity to about 200 Ω·m marked by the dashed red line in Figure 8. This change is interpreted to represent the lithosphere-asthenosphere boundary (*see* Jones, 1999; Eaton et al., 2009). At depths of 50–200 km, in the region beneath the southern extent of the Penrhyn Group there is a distinct decrease in the overall apparent resistivity (~300 Ω·m) of the mantle lithosphere compared to the neighbouring resistive mantle. Although there is limited sensitivity in this region, model testing shows that a change from lower resistivities beneath sites mel019, and mel018 to high resistivities beneath southernmost extent of the profile is robust and required by the data. Laboratory tests have shown that conductivity increases with increasing water content in olivine (Yoshino et al., 2009). This explanation for reduced resistivities requires a mechanism for hydrating olivine and sustaining the water content over long periods of time. This zone of lowered resistivity lies directly beneath the near-vertical conductive feature in Figure 6c, suggesting that this fault may be a major shear zone that extends into the upper mantle separating the Repulse Bay Block to the south from the northern Rae Craton units. It has been shown in laboratories that there is an inverse relationship between the electrical resistivity of mantle olivine and its grain size, where a substantial decrease in grain size can decrease the resistivity by up to two orders of magnitude (ten Grotenhuis et al., 2004). The northward lateral extend of this low-resistivity zone, however, is uncertain due to the shielding effect on the data recorded in the vicinity of the Penryhn Group. It is possible that the upper mantle beneath the exposed Penrhyn Group has lower resistivity values (~500 Ω·m) associated with Paleoproterozoic juvenile mantle, as imaged beneath the Baffin Island survey (Evans et al., 2005).

CONCLUSIONS

Distortion and strike analysis suggest that the northernmost sites have two distinct anisotropic layers. The data in the period range that corresponds to crustal depths have a preferred geoelectric strike direction of +99°, likely an influence of the abundant east-west faulting. At greater periods (deeper depths) for the northernmost sites, and all periods for the southern sites, the geoelectric strike direction is +34°, similar to that of the regional geology. This suggest coupling between the crust and the mantle, where the strike direction in the northern half of the profile is influenced solely by late-stage faulting that has limited penetration into the upper mantle.

In general, the variably reworked Archean Rae Craton to the north is highly resistive (>10 000 Ω·m), however less resistive (~5000 Ω·m) near vertical structures that extend to the base of the crust are imaged and interpreted to represent the subsurface expression of the east-trending faults. Extremely low resistivities (<10 Ω·m) are associated with the Paleoproterozoic supractrustal metasedimentary rocks of the Penrhyn Group, limiting the penetration beneath the geophysically mapped units. A comparison between apparent resistivity and phase-response curves between sites recorded on highly resistive Archean crust and less resistive Paleoproterozoic supracrustal rocks indicate that the exposed bands of Archean basement material with the Fox fold belt are underlain by low resistivities typical of the Penhryn Group metasedimentary units. A decrease in resistivity of two orders of magnitude is observed between 36–39 km over most of the profile, and is interpreted as the crust-mantle boundary.

Beneath the Rae Craton, a thickened resistive upper mantle is observed to depths of about 200 km where a decrease in resistivity is interpreted to represent the lithosphere-asthenosphere boundary. At depths of 70–200 km toward the south end of the profile there is a change from moderate resistivities (~300 Ω·m) to high-resistivity values (~3000 Ω·m) from north to south across the mapped surface trace of a shear zone at the southernmost extent of the Paleoproterozoic units. This suggests changes in the mantle structure or composition between the Repulse Bay Block to the south and the Rae Craton to the north.

The magnetotelluric method has been demonstrated to aid significantly in area selection for potential diamondiferous provinces (Jones and Craven, 2004; Jones et al., 2009b). In terms of diamond potential for the Melville Peninsula, the results here suggest that the central part of the peninsula may be too thin to support diamonds in its roots, much like the Rehoboth Terrane in Botswana (Muller et al., 2009). The northern part of the peninsula exhibits a lithosphere of some 200 km thickness extent, so the lower lithosphere is well within the diamond stability field. To the south it is not possible to be definitive, due to the presence of the Penrhyn Group sedimentary rocks. Very long period MT (VLMT) measurements need to be acquired in this area in order to obtain information about the lithospheric mantle.

ACKNOWLEDGMENTS

This work was funded by Natural Resources Canada under the Geo-mapping for Energy and Minerals (GEM) Program. The authors would like to acknowledge B. Roberts and A. Rafeek for help in generating some of the figures and T. Skulski for providing detailed geological information. Internal review of the manuscript was provided by J. Craven.

REFERENCES

Berman, R.G., Sandborn-Barrie, M., Stern, R.A., and Carson, C.J., 2005. Tectonometamorphism at ca. 2.35 and 1.85 Ga in the Rae Domain, western Churchill Province, Nunavut, Canada: insights from structural, metamorphic and in situ geochronological analysis of the southwestern Committee Bay belt; Canadian Mineralogist, v. 43, p. 409–442. doi:10.2113/gscanmin.43.1.409

Blackadar, R.G., 1958. Fury and Hecla Strait, District of Franklin, Northwest Territories; Geological Survey of Canada, Preliminary Map 3-1958, scale 1:506 880. doi:10.4095/108560

Boerner, D.E., Kurtz, R.D., Craven, J.A., Ross, G.M., Jones, F.W., and Davis, W.J., 1999. Electrical conductivity in the Precambrian lithosphere of Western Canada; Science, v. 283, p. 668–670. doi:10.1126/science.283.5402.668

Bostick, E.X., 1977. A simple almost exact method of MT analysis; Workshop on Electrical Methods in Geothermal Exploration, U.S. Geological Survey, Contract No. 14080001–8-359, p. 174–183.

Cagniard, L., 1953. Basic theory of the magnetotelluric method of geophysical prospecting; Geophysics, v. 18, p. 605–635. doi:10.1190/1.1437915

Chave, A.D. and Thomson, D.J., 2004. Bounded influence magnetotelluric response function estimation; Geophysical Journal International, v. 157, p. 988–1006. doi:10.1111/j.1365-246X.2004.02203.x

Corrigan, D., Pehrsson, S., Wodicka, N., and de Kemp, E., 2009. The Paleoproterozoic Trans-Hudson Orogen: a prototype of modern accretionary processes; *in* Ancient Orogens and Modern Analogues, (ed.) J.B. Murphy, J.D. Keppie, and A.J. Hynes; Geological Society, London, Special Publications, v. 327, p. 457–479.

Duba, L. and Shankland, T.J., 1982. Free carbon and electrical conductivity in the Earth's mantle; Geophysical Research Letters, v. 9, p. 1271–1274. doi:10.1029/GL009i011p01271

Ducea, M.N. and Park, S.K., 2000. Enhanced mantle conductivity from sulfide minerals, southern Sierra Nevada, California; Geophysical Research Letters, v. 27, p. 2405–2408. doi:10.1029/2000GL011565

Eaton, D.W., Darbyshire, F., Evans, R.L., Grutter, H., Jones, A.G., and Yuan, X., 2009. The elusive lithosphere-asthenosphere boundary (LAB) beneath cratons; Lithos, v. 109, p. 1–22. doi:10.1016/j.lithos.2008.05.009.

Erdmann, S., Wodicka, N., Jackson, S.E., and Corrigan, D., 2013. Zircon textures and composition: refractory recorders of magmatic volatile evolution; Contributions to Mineralogy and Petrology, v. 165, p. 45–71. doi:10.1007/s00410-012-0791-z

Evans, S., Jones, A.G., Spratt, J., and Katsube, J., 2003. Central Baffin electromagnetic experiment (CBEX), Phase 2; Geological Survey of Canada, Current Research 2003-C24, 10 p. doi:10.4095/214206

Evans, S., Jones, A.G., Spratt, J., and Katsube, J., 2005. Central Baffin electomagnetic experiment (CBEX) maps the NACP in the Canadian arctic; Physics of the Earth and Planetary Interiors, v. 150, p. 107–122. doi:10.1016/j.pepi.2004.08.032

Frisch, T., 1980. Tonalite gneisses, western Melville Peninsula, District of Franklin; Geological Survey of Canada, Current Research, Paper 80-1C p. 217–219.

Glover, P.W.J., Pous, J., Queralt, P., Munoz, J.-A., Liesa, M., and Hole, M.J., 2000. Integrated two-dimensional lithospheric conductivity modeling in the Pyrenees using field-scale and laboratory measurements; Earth and Planetary Science Letters, v. 178, p. 59–72. doi:10.1016/S0012-821X(00)00066-2

Groom, R.W. and Bailey, R.C., 1989. Decomposition of magnetotelluric impedance tensors in the presence of local three-dimensional galvanic distortion; Journal of Geophysical Research, v. 94, p. 1913–1925. doi:10.1029/JB094iB02p01913

Haak, V. and Hutton, V.R.S., 1986. Electrical resistivity in continental lower crust; Geological Society of London; Special Publication, v. 24, p. 35–49. doi:10.1144/GSL.SP.1986.024.01.05

Henderson, J.R., 1983. Structure and metamorphism of the Aphebian Penrhyn Group and its Archean basement complex in the Lyon inlet area, Melville Peninsula, District of Franklin; Geological Survey of Canada, Bulletin 324, 50 p.

Jones, A.G., 1983. On the equivalence of the "Niblett'" and "Bostick'" transformations in the magnetotelluric method; Journal of Geophysics, v. 53, p. 72–73.

Jones, A.G., 1992. Electrical conductivity of the continental lower crust; Chapter 3 *in* Continental Lower Crust, (ed.) D.M. Fountain, R.J. Arculus, and R.W. Kay, Elsevier, Amsterdam, The Netherlands, p. 81–143.

Jones, A.G., 1999. Imaging the continental upper mantle using electromagnetic methods; Lithos, v. 48, p. 57–80. doi:10.1016/S0024-4937(99)00022-5

Jones, A.G., 2006. Electromagnetic interrogation of the anisotropic Earth: Looking into the Earth with polarized spectacles; Physics of the Earth and Planetary Interiors, v. 158, p. 281–291. doi:10.1016/j.pepi.2006.03.026

Jones, A.G. and Craven, J.A., 2004. Area selection for diamond exploration using deep-probing electromagnetic surveying; Lithos, v. 77, p. 765–782. doi:10.1016/j.lithos.2004.03.057

Jones, A.G. and Ferguson, I.J., 2001. The electric Moho; Nature, v. 409, p. 331–333. doi:10.1038/35053053

Jones, A.G. and Jödicke, H., 1984: Magnetotelluric transfer function estimation improvement by a coherence-based rejection technique; *in* Abstract volume, 54th Society of Exploration Geophysics Annual General Meeting, Atlanta, Georgia, 2–6 December, p. 51–55.

Jones, A.G. and Spratt, J.E., 2001. A simple method for deriving the uniform field MT responses in auroral zones; Earth and Planetary Science Letters, v. 54, p. 443–450.

Jones, A.G., Chave, A.D., Auld, D., Bahr, K., and Egbert, G., 1989. A comparison of techniques for magnetotelluric response function estimation; Journal of Geophysical Research, v. 94, p. 14 201–14 213.

Jones, A.G., Snyder, D., Hanmer, S., Asudeh, I., White, D., Eaton, D., and Clarke, G., 2002. Magnetotelluric and teleseismic study across the Snowbird Tectonic Zone, Canadian Shield: a Neoarchean mantle suture? Geophysical Research Letters, v. 29, no. 17, p. 10-1–10-4, doi:10.1029/2002GL015359.

Jones, A.G., Lezaeta, P., Ferguson, I.J., Chave, A.D., Evans, R., Garcia, X., and Spratt, J., 2003. The electrical structure of the Slave craton; Lithos, v. 71, p. 505–527. doi:10.1016/j.lithos.2003.08.001

Jones, A.G., Evans, R.L., and Eaton, D.W., 2009a. Velocity-conductivity relationships for mantle mineral assemblages in Archean cratonic lithosphere based on a review of laboratory data and Hashin-Shtrikman extremal bounds; *in* Special Issue of Lithos Devoted to The Structure of the Lithosphere: the petro-geophysical approach workshop that was held in Merrickville, Ontario, 7–10 March 2007; Lithos, v. 109, p. 131–143. doi:10.1016/j.lithos.2008.10.014.

Jones, A.G., Evans, R.L., Muller, M.R., Hamilton, M.P., Miensopust, M.P., Garcia, X., Cole, P., Ngwisanyi, T., Hutchins, D., Fourie, C.J.S, Jelsma, H., Aravanis, T., Pettit, W., Webb, S., Wasborg, J., and The SAMTEX Team, 2009b. Area selection for diamonds using magnetotellurics: examples from southern Africa; Lithos, v. 112, p. 83–92. doi:10.1016/j.lithos.2009.06.011

Korja, T., 2007. How is the European lithosphere imaged by magnetotellurics; Surveys in Geophysics, v. 28, p. 239–272. doi:10.1007/s10712-007-9024-9

Laflamme, C., 2011. New constraints on Paleoproterozoic metamorphism affecting the Repulse Bay block, Melville Peninsula, Nunavut: in situ LA-ICPMS from two generations of Monazite growth; *in* Abstract Volume, Geological Association of Canada–Mineralogical Association of Canada Annual Meeting, May 24–27, 2011, Ottawa, Ontario.

LeCheminant, A.N., Roddick, J.C., Tessier, A.C., and Bethune, K.M., 1987. Geology and U-Pb ages of Early Proterozoic calc-alkaline plutons northwest of Wager Bay, District of Keewatin; *in* Current Research, Part A; Geological Survey of Canada, Paper 87-1A, p. 773–782.

Marquis, G., Jones, A.G., and Hyndman, R.D., 1995. Coincident conductive and reflective lower crust across a thermal boundary in southern British Columbia, Canada; Geophysical Journal International, v. 120, p. 111–131. doi:10.1111/j.1365-246X.1995.tb05915.x

McNeice, G.W. and Jones, A.G., 2001. Multisite, multifrequency tensor decomposition of magnetotelluric data; Geophysics, v. 66, p. 158–173. doi:10.1190/1.1444891

Muller, M.R., Jones, A.G., Evans, R.L., Grütter, H.S., Hatton, C., Garcia, X., Hamilton, M.P., Miensopust, M.P., Cole, P., Ngwisany, T., Hutchins, D., Fourie, C.J., Jelsma, H., Aravanis, T., Pettit, W., Webb, S.J., Wasborg, J., and The SAMTEX Team, 2009. Lithospheric structure, evolution and diamond prospectivity of the Rehoboth Terrane and western Kaapvaal Craton, southern Africa: constraints from broadband magnetotellurics; Lithos, v. 112, p. 93–105. doi:10.1016/j.lithos.2009.06.023

Niblett, E.R. and Sayn-Wittgenstein, C., 1960. Variation of electrical conductivity with depth by the magnetotelluric method; Geophysics, v. 25, p. 998–1008. doi:10.1190/1.1438799

Poe, B.T., Romano, C., Nestola, F., and Smyth, J.R., 2010. Electrical conductivity anisotropy of dry and hydrous olivine at 8 GPs; Physics of the Earth and Planetary Interiors, v. 181, p. 103–111. doi:10.1016/j.pepi.2010.05.003

Schau, M. and Heywood, W.W., 1984. Geology of northern Melville Peninsula; Geological Survey of Canada, Open File 1046, scale 1:500 000. doi:10.4095/129843

Schmucker, U., 1970. Anomalies of geomagnetic variations in the Southwestern United States; Bulletin of Scripps Institute of Oceanography, University of California Press, v. 13, p. 165.

Spratt, J.E., Jones, A.G., Jackson, V., Collins, L., and Avdeeva, A., 2009. Lithospheric geometry of the Wopmay Orogen from a Slave Craton to Bear Province magnetotelluric transect; Journal of Geophysical Research, v. 114, issue B1. doi:10.1029/2007JB005326.

ten Grotenhuis, S.M., Drury, M.R., Peach, C.J., and Spiers, C.J., 2004. Electrical properties of fine-grained olivine: evidence for grain boundary transport; Journal of Geophysical Research, v. 109, issue B6. doi:10.1029/2003JB002799.

Wait, J.R., 1962. Theory of magnetotelluric fields, Journal of Research of the National Bureau of Standards - D; Radio Propagation, v. 66d, p. 509–541.

Wu, X., Ferguson, I.J., and Jones, A.G., 2002. Magnetotelluric response and geoelectric structure of the Great Slave Lake shear zone; Earth and Planetary Science Letters, v. 196, p. 35–50. doi:10.1016/S0012-821X(01)00594-5

Yoshino, T., Matuszaki, T., Shatskiy, A., and Katsura, T., 2009. The effect of water on the electrical conductivity of olivine aggregates and its implications for the electrical structure of the upper mantle; Earth and Planetary Science Letters, v. 288, p. 291–300. doi:10.1016/j.epsl.2009.09.032

Geological Survey of Canada Project MGM008